

Article

Sustainable Management of Autoclaved Aerated Concrete Wastes in Gypsum Composites

Fabio Iucolano , Assunta Campanile, Domenico Caputo  and Barbara Liguori 

Department of Chemical, Materials and Production Engineering (DICMaPI), University of Naples Federico II, 80125 Naples, Italy; assunta.campanile@unina.it (A.C.); domenico.caputo@unina.it (D.C.); barbara.liguori@unina.it (B.L.)

* Correspondence: fabio.iucolano@unina.it

Abstract: Promoting the use of gypsum and gypsum-based materials in construction is a successful strategy from an environmental point of view; it allows a lower energy demand with a sensible reduction in carbon dioxide emissions. At the same time, the manufacturing of gypsum products can represent an interesting sector to redirect and manage the large amount of autoclaved aerated concrete (AAC) waste. In this paper a sustainable application of AAC granulate waste in gypsum-based building materials was proposed. The intrinsic compatibility derived their chemical composition and allowed it to partially substitute raw gypsum with the waste up to 30% without affecting the functional and structural properties of the final product. Physical characterization and sound absorption data confirmed that the addition of AAC waste does not significantly alter the typical porosity of the gypsum composite. Finally, all of the composites reached mechanical performances suitable for different building application as gypsum plaster.



Citation: Iucolano, F.; Campanile, A.; Caputo, D.; Liguori, B. Sustainable Management of Autoclaved Aerated Concrete Wastes in Gypsum Composites. *Sustainability* **2021**, *13*, 3961. <https://doi.org/10.3390/su13073961>

Academic Editor: Ilaria Capasso, Giuseppe Brando and Gianluca Iezzi

Received: 10 March 2021
Accepted: 29 March 2021
Published: 2 April 2021

Publisher's Note: MDPI stays neutral with regard to jurisdictional claims in published maps and institutional affiliations.



Copyright: © 2021 by the authors. Licensee MDPI, Basel, Switzerland. This article is an open access article distributed under the terms and conditions of the Creative Commons Attribution (CC BY) license (<https://creativecommons.org/licenses/by/4.0/>).

Keywords: autoclaved aerated concrete; lightweight aggregates; plaster; gypsum

1. Introduction

Huge quantities of natural resources are consumed every year by the building industry and, at the same time, a significant amount of construction and demolition waste (CDW) is generated. One of the main challenges of the manufacturers is the implementation of measures to move towards a circular economy industry which, coupled to an efficient resource recovery system, leads to environmental and economic advantages [1,2]. Autoclaved aerated concrete (AAC) arises from the need to obtain a light, prepacked material, with the same physical and mechanical properties as a compact product. The massive growth of autoclaved aerated concrete (AAC) application in the building industry, started in the 1940 in Europe, provides a large amount of AAC waste (AACW) in recent years.

The disposal of AACW to landfills, instead of being reused and recycled in new construction, may cause environmental problems, such as contaminant leaching and pH changes in the surrounding soil and water [3].

The market related to AAC production is estimated at 6.32 billion of dollars in 2016 and is expected to reach 10.98 billion of dollars by 2023 [4]. Advanced characteristics of autoclaved aerated concrete and the rising importance of green buildings are some of the key factors influencing the market growth. The exceptional characteristics of AAC are due to its porous closed-cell structure generated by the reaction between the alkaline components of the cement and a foaming agent, the aluminum powder. To promote the crystallization of calcium silicate hydrate phases (particularly tobermorite), a significant amount (2–5%) of calcium sulphate in the form of gypsum or anhydrite is added to the raw materials [5,6]. Therefore, the chemical composition of AAC waste can represent an important limit in its recycling since sulfate compounds can cause severe technical problems, such as efflorescence and internal sulfate attack, and environmental effects (salinity, sulfide formation, eutrophication) which are caused by leaching on groundwater [7].

Recently, some authors proposed different recycling options for AAC waste, such as replacement of the sand fraction in the production of new AAC, for raw material for Portland clinker production, and oil and gas absorbance [7–10].

As principal constituents, gypsum-based products contain three different forms of calcium sulphate: dihydrate ($\text{CaSO}_4 \cdot 2\text{H}_2\text{O}$), hemihydrate ($\text{CaSO}_4 \cdot 0.5\text{H}_2\text{O}$), and anhydrite (CaSO_4). They are lightweight, have excellent moldability, fire resistance, and sound absorption. Gypsum offers several applications as building material, such as prefabricated products (dry wallboards, ceiling panels, flooring panels), blocks and panels for partitions and internal walls, as well as interior plasters. Finally, gypsum products have been successfully used as sound and heat-insulating materials [11–14].

Nowadays, the use of gypsum in construction is relatively limited, despite the low price of raw material and general recognition of gypsum as environmental-friendly material [15]. Differing from interior plasters and plasterboards, a promising use of gypsum can be in lightweight products that are either chemically foaming the plaster or using a light aggregate [16,17]. Promoting the application of gypsum in construction can represent an important environmental issue since it allows for a lower energy demand due to lower raw material calcination temperatures with a sensible reduction in carbon dioxide emissions [16]. Although several studies have been published on gypsum-based composites using different kinds of wastes [17–21], no previous study has been found in which AAC waste has been used as an aggregate in gypsum composite. Due to an intrinsic compatibility deriving from their chemical composition, AAC wastes can be used to partially substitute raw gypsum in the manufacture of gypsum-based products. Furthermore, incorporating these fillers in a gypsum composite reduces the amount of raw material used for its manufacture and represents an improvement over gypsums without additions.

The incorporation of waste particles in a gypsum composite can alter all of the processes involving in the consolidation of the binder. First, a complete characterization of the AAC waste was carried out in order to verify its compatibility with gypsum manufacture. Then, the effect of AAC wastes was studied either on the setting process of the gypsum product or their structural and functional properties.

2. Materials and Methods

2.1. Materials

In the present investigation, gypsum produced by Gyproc Saint-Gobain (Milano, Italy), mainly constituted by calcium sulphate hemihydrate, was used. AAC granules were provided by Bacchi Spa and were derived from the cellular concrete blocks (named GasBeton Evolution, specific gravity = 0.48 g/cm^3).

The mineralogical composition of the raw materials was carried out by X-ray diffractometry (X'Pert Pro diffractometer, PANalytical) with the following test conditions: Cu $K\alpha$ radiation, 2θ interval: $5\text{--}60^\circ$ range, step $0.02^\circ 2\theta$; $0.02^\circ 2\theta/\text{s}$; scan speed; slide opening 0.5. The morphology of each sample was analyzed by scanning electron microscopy (SEM) (Cambridge S440 Scanning Electron Microscope, Bullard Laboratories, Cambridge, UK).

The thermal behavior was investigated by thermogravimetric analysis (Netzsch, model 409ST Luxx) in the temperature range of 20 to 1200°C with a heating rate of $10^\circ\text{C}/\text{min}$.

The grain size distribution of the AAC waste was obtained by dry sieving according to the European standard UNI EN 933-1:2012.

Light and porous aggregates can absorb large quantities of mixing water influencing the water/binder ratio, and negatively affect mechanical behavior. The water-absorption capacity was preventively evaluated according to UNI EN 1097-6:2013.

2.2. AAC–Gypsum Composites Preparation and Characterization

Three gypsum mixtures were manufactured by replacing gypsum with 10, 20, and 30 wt% of AAC waste (called GBET10, GBET20, and GBET30), respectively. A reference gypsum sample (REF), without waste, was also produced. Gypsum and waste aggregates

were dry mixed and poured in a suitable amount of water in a planetary mixer. A liquid to solid ratio of 0.7 was selected for manufacturing all the specimens.

Finally, the mixtures were cast in three different molds: $40 \times 40 \times 160$ mm prisms for mechanical tests, $125 \times 125 \times 20$ mm slabs for vapor permeability tests, and 100×20 mm disks for acoustic tests (Figure 1).

The gypsum composites were dried for 48 h at 40°C and placed in a climatic chamber at 20°C and 50% RH until the time of testing. All of the specimens were produced in triplicate.

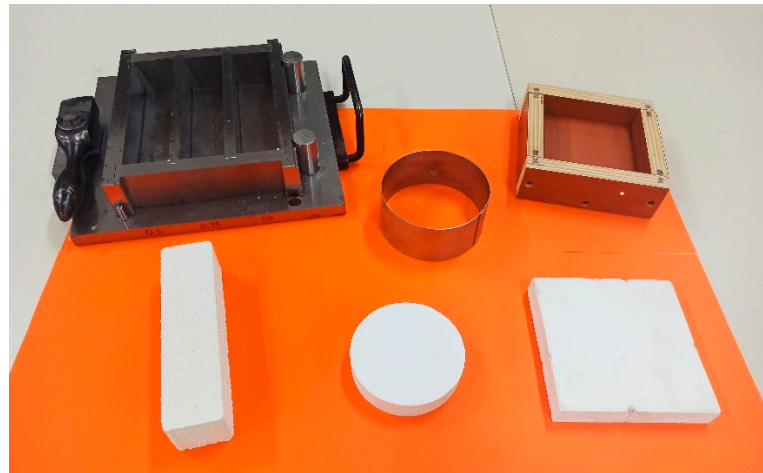


Figure 1. Samples geometry ($40 \times 40 \times 160$ mm) for mechanical tests (**left**), acoustic test (100×20 mm) (**centre**), and for vapor permeability tests ($125 \times 125 \times 20$ mm) (**right**).

The morphological characterization of gypsum composites was performed by scanning electron microscopy (SEM).

In order to check the influence of the AAC wastes in addition to the gypsum composites, the density, or the open porosity and the water vapor permeability, were evaluated. The real density and the open porosity were evaluated according to the European Standard UNI 11060:2003. The specimens were immersed in water under a vacuum at room temperature for two hours. After that, they were weighted (bulk and hydrostatic weight). Real density was evaluated by the pycnometer method.

The water vapor permeability was evaluated according to the European Standard UNI EN 1015-19:2008. The samples were placed in plexiglass vessels over a saturated solution of potassium nitrate (KNO_3) and were able to maintain a constant relative humidity (RH) of 93.2% at $T = 20^\circ\text{C}$. Then, the containers were sealed and placed in a climatic chamber at $T = 20 \pm 2^\circ\text{C}$ and $\text{RH} = 50 \pm 5\%$. The water vapor flow through the specimen was evaluated by measuring, every 24 h, the mass change of the vessels. The test is considered completed when the above mass change is constant for at least three consecutive weights which is the quantity of water vapor passing through the sample per unit when the time is constant.

By processing the data obtained from the test, it is possible to calculate the water vapor permeability:

$$W_{vp} = \Delta \cdot t \quad (1)$$

where Δ is the average value of the permeation to water vapor [$\text{kg}/\text{m}^2 \cdot \text{s} \cdot \text{Pa}$], and t is the thickness of the samples [m].

Moreover, further parameters were evaluated according to the European Standard UNI EN 12086:2013:

(a) the resistance factor to the diffusion of water vapor (μ) which allows for the relative resistance of the material to be overpassed by the vapor, and it is equal to:

$$\mu = \frac{\delta_{air}}{\delta} \quad (2)$$

where δ_{air} is the permeability of water vapor in the air [kg/m·s·Pa], and δ is the permeability of water vapor in the sample [kg/m·s·Pa];

(b) the thickness of the equivalent air layer (s_d) which indicates the thickness of the still air layer and offers the same resistance to the diffusion of water vapor of the examined material, and it is equal to:

$$s_d = \mu \cdot d \quad (3)$$

where μ is the resistance factor to the diffusion of water vapor, and d is the thickness of the sample [m].

Mechanical characterization was performed by three-point flexural and compressive test (UNI EN 1015-11:2019). The three-point flexural test was carried out using a Tensometer 2020 device by Alpha Technologies with a 10 kN load cell and a crossbar lowering speed of 0.5 mm/min. On each of the two parts of samples obtained from the flexure test, the compression test was also performed using the same Tensometer 2020 device with a 50 kN load cell and a crossbar lowering speed of 1 mm/min. All tests were carried out in triplicate.

Finally, a preliminary investigation of the acoustic absorption coefficient for normal incidence (α) was carried out on disk-shaped specimens at room conditions.

This coefficient represents the ratio between the absorbed sound energy and the incident sound energy and is now considered an important feature of building material. The measurements were carried out following the standard UNI EN 10534-2:2001 by means of a 570 mm long Kundt tube with an internal diameter equal to 100 mm. A generator of low frequency stationary waves (frequencies ranging in the range 200–2.000 Hz) was placed at one end of the tube, while the specimen was fixed at the opposite side of the tube. Moreover, two microphones, which were 50 mm far from each other, were placed in the tube with the first one at 200 mm away from the sample.

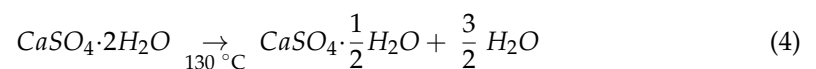
3. Results and Discussion

3.1. Evaluation of the AAC Granulates Waste

Grain size distribution of the granules, reported in Figure 2, was obtained by mechanical sieving according to European Standards UNI EN 933-1:2012. To avoid the presence of overly coarse aggregates inside the composites, only the fraction within the range 0 ÷ 2 mm was used in the present investigation. Water absorption of 72.5 wt.% and a bulk mass of 0.86 g/cm³ for the AAC granules were obtained by the pycnometer method.

Figure 3a shows the porous structure of the AAC granules and its mineralogical composition were obtained by means of the XRD analysis (Figure 3b). The XRD pattern showed the presence of tobermorite (ICDD 01–083–1520), quartz (ICDD 00–046–1045), gypsum (ICDD 00–036–0432), and calcite (ICDD 01–086–2339) as the main crystalline phases.

Inspecting the thermal behavior of AAC granules, two endothermic effects (Figure 4) were detected: the first peak at 130 °C represented the decomposition of the gypsum:



Between 200 and 500 °C, the gradual weight loss was due to decomposition of the calcium silicate hydrated phase (CSH, tobermorite); then, at around 570 °C the dehydroxylation of calcium hydroxide appeared. Finally, the peak at 745 °C indicated the decomposition of calcium carbonate.

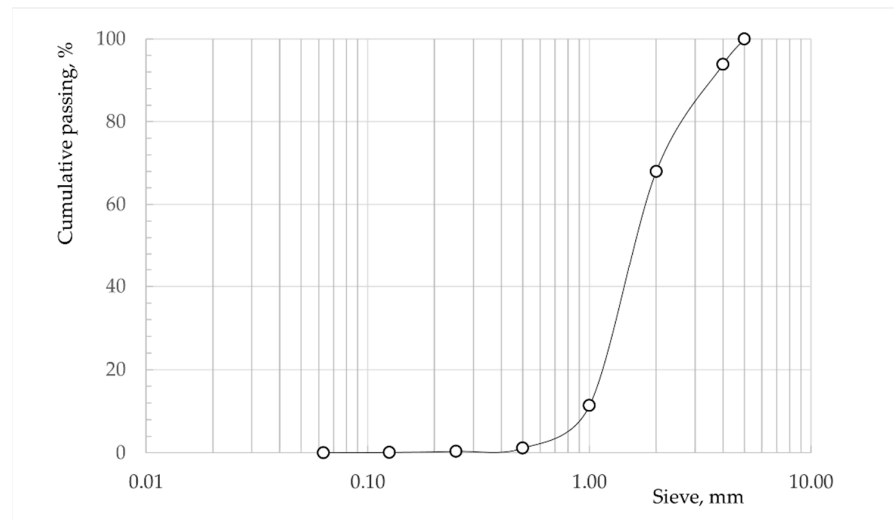


Figure 2. Grain size distribution of AAC granules.

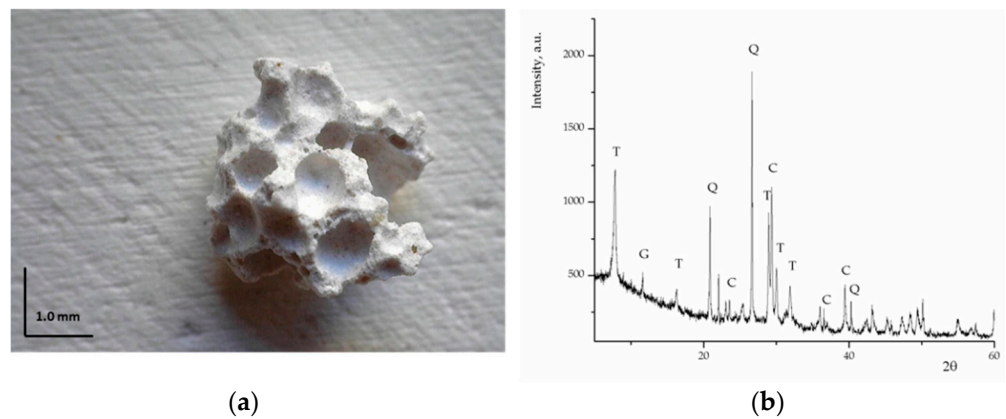


Figure 3. (a) Optical image (40×) and (b) XRD pattern of the AAC granulates (T = tobermorite; G = gypsum; Q = quartz; C = calcite).

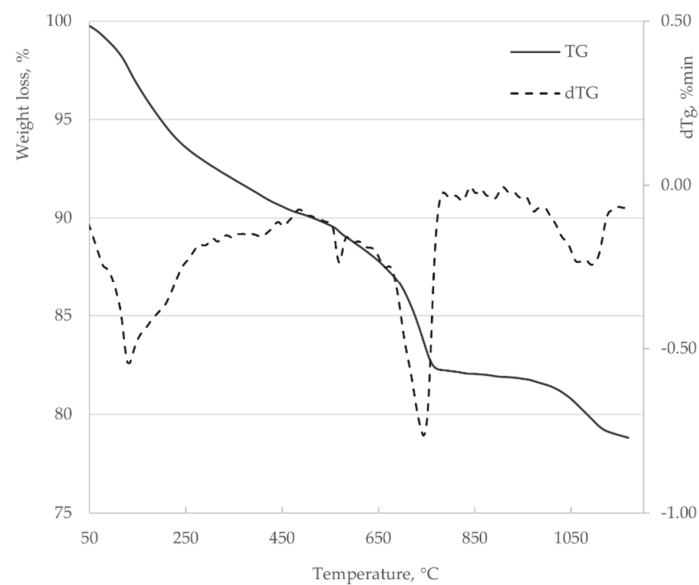


Figure 4. TG/DTA curve of AAC waste.

3.2. AAC–Gypsum Composites Characterization

Figure 5 shows the sections of all the prismatic samples ($40 \times 40 \times 160$ mm) which are suitably cut and smoothed.

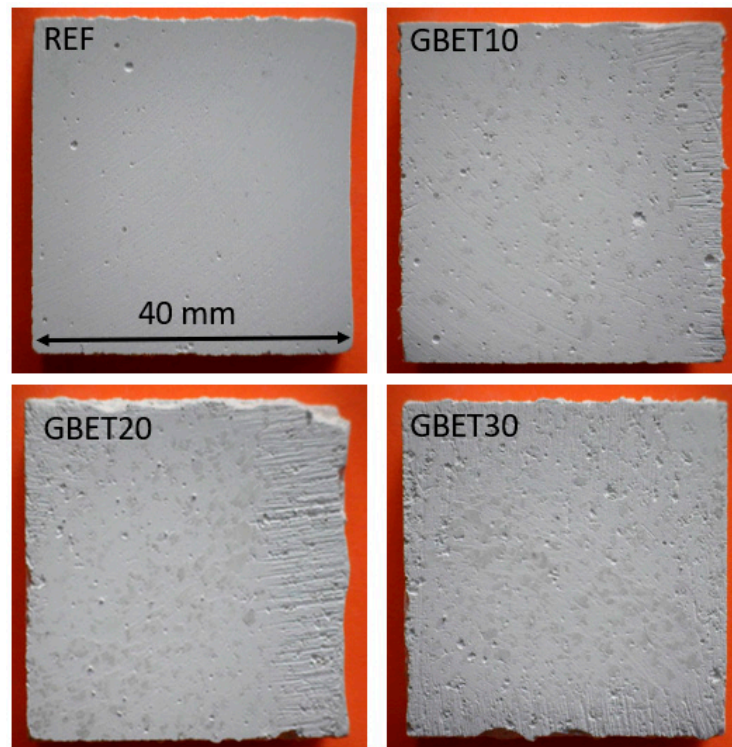


Figure 5. Surfaces of the sections of all the manufactured specimens.

The presence of AAC waste led to a chromatic variation on the surfaces of the sections, where some light grey spots were more visible when higher was the amount of granules substitution. This presence was further evidenced in Figure 6, where a magnification of GBET30 section's surface was reported. Both the figures indicate that the AAC granules were homogeneously distributed within the samples and adhered well to the gypsum.

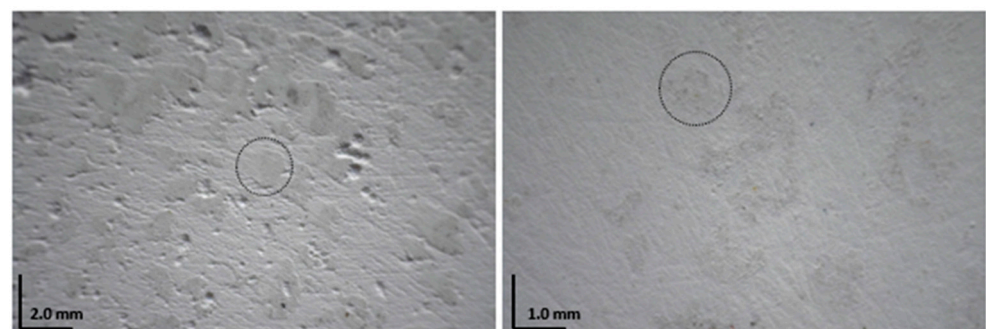


Figure 6. AAC granules on section's surface of GBET30 sample.

SEM images (150X magnification, Figure 7) of the fracture surfaces of all of the manufactured samples showed that the addition of the AAC waste resulted in a modification of the morphology of the matrix which appeared rather compact for the reference sample (REF) and gradually more porous when increasing the AAC addition. In the range of investigated compositions (0–30%), the substitution of the gypsum with aerated aggregates led to a change in the morphology of the binder matrix, primarily regarding the size and shape of the pores.

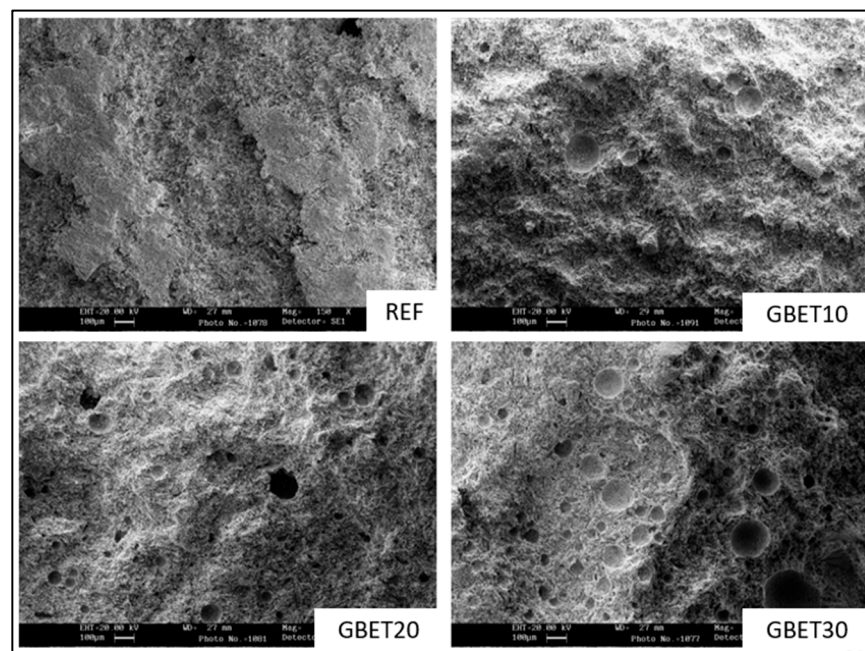


Figure 7. Morphological aspect of the fracture surfaces of different samples.

The addition of AAC waste slightly increased the open porosity and, consequently, the real density slightly decreased. Therefore, the mechanical properties of gypsum samples, in terms of compression and flexural resistance, were also affected as reported in Table 1. Plotting the strength values vs. the number of aggregates (Figure 8), both resistances exhibited an inversely proportional dependence with the percentage of AAC granules with a maximum reduction (in correspondence of GBET30 sample) that was less than 10% with respect to the resistances of the reference sample.

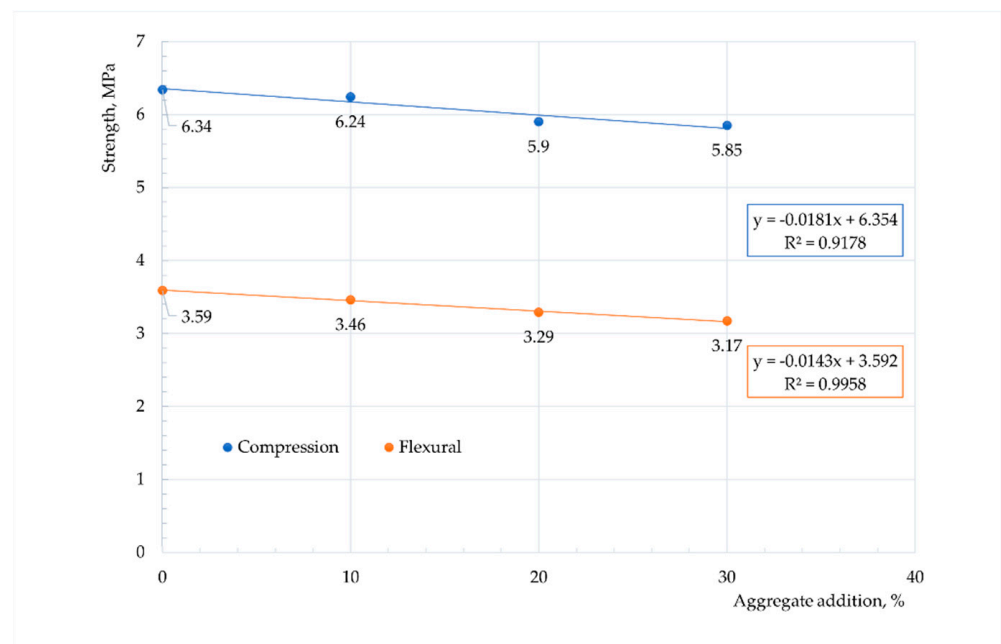


Figure 8. Linear dependence of mechanical properties with AAC granules addition.

Table 1. Physical and mechanical properties of gypsum composites.

Sample	Real Density [g/mL]	Open Porosity [%]	Compressive Strength [MPa]	Flexural Strength [MPa]
REF	2.23 ± 0.01	51.12 ± 0.13	6.34 ± 0.24	3.59 ± 0.03
GBET10	2.15 ± 0.01	51.57 ± 0.17	6.24 ± 0.16	3.46 ± 0.18
GBET20	2.09 ± 0.02	52.14 ± 0.16	5.90 ± 0.22	3.29 ± 0.13
GBET30	2.07 ± 0.01	52.35 ± 0.18	5.85 ± 0.28	3.17 ± 0.04

The BS EN 13279-1:2018 European Standard specifies the characteristics and performance of gypsum binders for different building purposes for direct use on site and for further processing into gypsum blocks, plasterboards, boards with fibrous reinforcement, fibrous plasterwork, and ceiling elements (Table 2).

Table 2. Specifications for gypsum in construction.

Type	Flexural Strength [N/mm ²]	Compressive Strength [N/mm ²]
B1-Gypsum for construction ^a	≥1	≥2
B2-Gypsum mortar ^b	≥1	≥2
B3-Gypsum mortar with lime ^c	≥1	≥2
B4-Lightweight gypsum ^a	≥1	≥2
B5-Lightweight gypsum mortar ^b	≥1	≥2
B6-Lightweight gypsum mortar with lime ^c	≥1	≥2
B7-Lightweight gypsum for construction ^a	≥ 2	≥ 6

^a amount of gypsum ≥50%, ^b amount of gypsum <50%, ^c the amount of gypsum depends on whether gypsum alone (>50%) or gypsum mortar (<50%), in all cases, lime content is >5%.

Comparing the results of mechanical tests with the data reported in Table 2, all the mixtures performed in accordance with the specification for gypsum products in construction belonging to B1 to B6 categories. Only the GBET10 mixture respected the specifications provided for the B7 category (lightweight gypsum for construction).

These data confirmed the possibility of using a large amount of AAC wastes to produce a mixture suitable for several applications in the building sector. From now on, the samples that were richer in granules (GBET30) were selected and tested, following the procedure described in Section 2.2.

By processing the data obtained from the test, the factor of resistance to the diffusion of water vapor (μ), the thickness of the equivalent air layer (s_d), and the water vapor permeability (W_{vp}) of both samples were evaluated and reported in Table 3, with the respective standard deviations.

Table 3. Water vapor permeability behaviour of REF and GBET30 samples.

Sample	μ	s_d [m]	W_{vp} [kg m ⁻¹ s Pa]
REF	7.31 ± 0.28	0.16 ± 0.02	28.42 ± 0.99
GBET30	7.84 ± 0.19	0.17 ± 0.02	26.34 ± 1.14

According to previous data reported in the literature [22,23], the addition of macroporous particles, such as AAC waste aggregates, slightly increase the water vapor resistance factor. Thus, the slight increase of μ , s_d , and W_{vp} (Table 3) in the GBET30 sample was probably due to the macropore distribution of the AAC granules in the gypsum composites.

Accordingly, acoustic data reported in Figure 9 showed that the addition of 30% of AAC aggregate did not modify the acoustic absorption coefficient of the specimens which belongs to the range 0.04–0.1, depending on the signal frequency [24,25]. As the acoustic features of porous materials are strictly related to the size and typology of pores [17], it

can be argued that the presence of AAC aggregate does not significantly alter the typical porosity of the gypsum composites.

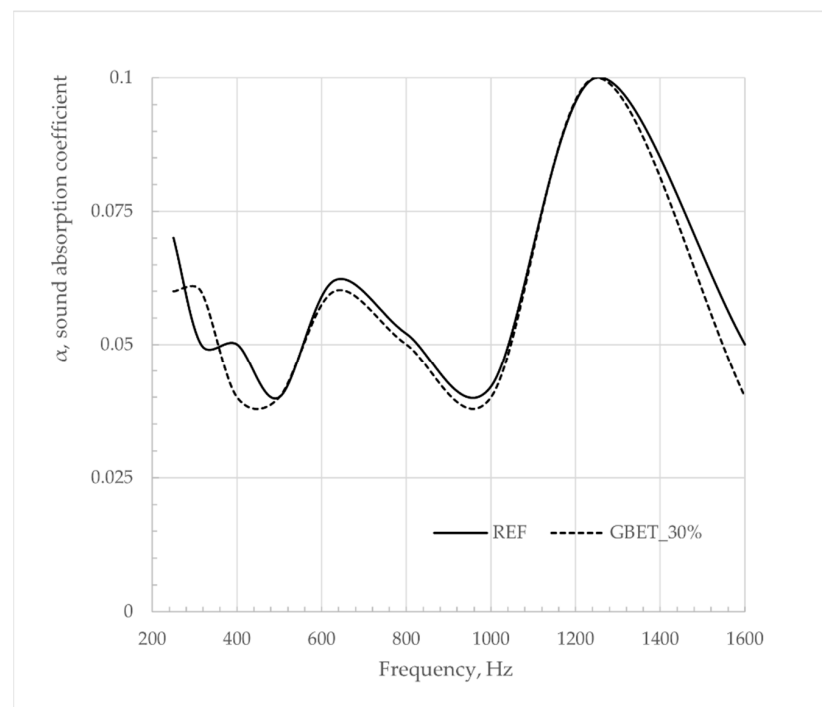


Figure 9. Sound absorption coefficient α as function of frequency for REF and GBET30 samples.

4. Conclusions

Gypsum manufacturing represents an interesting sector to redirect and manage a large amount of autoclaved aerated concrete waste. The paper deals with a characterization of this waste and is to be used as a partial substitution of raw gypsum in the manufacture of gypsum-based products.

The intrinsic chemical compatibility of AAC waste with gypsum resulted in a good interaction between added granules and gypsum which provided a homogeneous distribution and good adhesion of them within the gypsum composite. In the range of investigated compositions (0–30%), the substitution of gypsum with different percentages of waste aggregates (10, 20, and 30%) promoted a modification in the size and shape of the pores of the binder matrix. Slight increases in the open porosity affected the mechanical properties of the AAC–gypsum composites with a maximum reduction of about 10% with respect to the reference sample. Nevertheless, all the AAC–gypsum composites conform to the specifications for gypsum in construction and can be proposed for different building purposes for direct use on site or for further processing. As regards the functional properties, the addition of AAC waste has not significantly altered both the permeability and the sound absorption coefficient of the gypsum mixture. A further investigation could involve both the use of a higher amount of AAC replaced with gypsum and the role of this replacement on the thermal features of gypsum composites.

Author Contributions: Conceptualization, F.I. and B.L.; methodology, D.C.; validation, F.I.; investigation, A.C.; data curation, A.C. and F.I.; writing—original draft preparation, B.L. and A.C.; writing—review and editing, B.L., F.I.; supervision, D.C. All authors have read and agreed to the published version of the manuscript.

Funding: This research received no external funding.

Institutional Review Board Statement: Not applicable.

Informed Consent Statement: Informed consent was obtained from all subjects involved in the study.

Data Availability Statement: The data presented in this study are available on request from the corresponding author.

Acknowledgments: The authors are grateful to Rosario Romano for carrying out the acoustic characterization.

Conflicts of Interest: The authors declare no conflict of interest.

References

1. Jiménez-Rivero, A.; García-Navarro, J. Indicators to Measure the Management Performance of End-of-Life Gypsum: From Deconstruction to Production of Recycled Gypsum. *Waste Biomass Valorization* **2016**, *7*, 913–927. [[CrossRef](#)]
2. Accorsi, R.; Manzini, R.; Pini, C.; Penazzi, S. On the design of closed-loop networks for product life cycle management: Economic, environmental and geography considerations. *J. Transp. Geogr.* **2015**, *48*, 121–134. [[CrossRef](#)]
3. Ahmari, S.; Ren, X.; Toufigh, V.; Zhang, L. Production of geopolymeric binder from blended waste concrete powder and fly ash. *Constr. Build. Mater.* **2012**, *35*, 718–729. [[CrossRef](#)]
4. Fudge, C.; Fouad, F.; Klingner, R. Autoclaved aerated concrete. In *Developments in the Formulation and Reinforcement of Concrete*; Elsevier BV: Vancouver, BC, Canada, 2019; pp. 345–363.
5. Bergmans, J.; Nielsen, P.; Snellings, R.; Broos, K. Recycling of autoclaved aerated concrete in floor screeds: Sulfate leaching reduction by ettringite formation. *Constr. Build. Mater.* **2016**, *111*, 9–14. [[CrossRef](#)]
6. Schreiner, J.; Jansen, D.; Ectors, D.; Goetz-Neunhoeffler, F.; Neubauer, J.; Volkmann, S. New analytical possibilities for monitoring the phase development during the production of autoclaved aerated concrete. *Cem. Concr. Res.* **2018**, *107*, 247–252. [[CrossRef](#)]
7. Gyurkó, Z.; Jankus, B.; Fenyvesi, O.; Nemes, R. Sustainable applications for utilization the construction waste of aerated concrete. *J. Clean. Prod.* **2019**, *230*, 430–444. [[CrossRef](#)]
8. Hlawatsch, F.; Aycil, H.; Kropp, J. Autoclaved aerated concrete (AAC) rubble for new recycling building products: In dry premixed mortars for masonry, in masonry blocks, and in lightweight blocks. *ce/papers* **2018**, *2*, 457–464. [[CrossRef](#)]
9. Schoon, J.; De Buysser, K.; Van Driessche, I.; De Belie, N. Feasibility study on the use of cellular concrete as alternative raw material for Portland clinker production. *Constr. Build. Mater.* **2013**, *48*, 725–733. [[CrossRef](#)]
10. Lam, N.N. Recycling of AAC Waste in the Manufacture of Autoclaved Aerated Concrete in Vietnam. *Int. J. GEOMATE* **2021**, *20*, 128–134. [[CrossRef](#)]
11. Lushnikova, N.; Dvorkin, L. Sustainability of gypsum products as a construction material. *Sustain. Constr. Mater.* **2016**. [[CrossRef](#)]
12. Raghavendra, T.; Udayashankar, B. Engineering properties of controlled low strength materials using flyash and waste gypsum wall boards. *Constr. Build. Mater.* **2015**, *101*, 548–557. [[CrossRef](#)]
13. Guerra, B.C.; Bakchan, A.; Leite, F.; Faust, K.M. BIM-based automated construction waste estimation algorithms: The case of concrete and drywall waste streams. *Waste Manag.* **2019**, *87*, 825–832. [[CrossRef](#)] [[PubMed](#)]
14. Hansen, S.; Sadeghian, P. Recycled gypsum powder from waste drywalls combined with fly ash for partial cement replacement in concrete. *J. Clean. Prod.* **2020**, *274*, 122785. [[CrossRef](#)]
15. Vimmrová, A.; Keppert, M.; Svoboda, L.; Černý, R. Lightweight gypsum composites: Design strategies for multi-functionality. *Cem. Concr. Compos.* **2011**, *33*, 84–89. [[CrossRef](#)]
16. Fort, J.; Černý, R. Carbon footprint analysis of calcined gypsum production in the Czech Republic. *J. Clean. Prod.* **2018**, *177*, 795–802. [[CrossRef](#)]
17. Capasso, I.; Iucolano, F. Production of lightweight gypsum using a vegetal protein as foaming agent. *Mater. Struct.* **2020**, *53*, 1–13. [[CrossRef](#)]
18. Tounchuen, K.; Buggakupta, W.; Panpa, W. Characteristics of Automotive Glass Waste-Containing Gypsum Bodies Made from Used Plaster Mould. *Key Eng. Mater.* **2014**, *608*, 91–96. [[CrossRef](#)]
19. Alameda, L.; Calderón, V.; Junco, C.; Rodríguez, A.; Gadea, J.; Gutiérrez-González, S. Characterization of gypsum plasterboard with polyurethane foam waste reinforced with polypropylene fibers. *Mater. Constr.* **2016**, *66*, e100. [[CrossRef](#)]
20. Pedreño-Rojas, M.A.; Rodríguez-Liñán, C.; Flores-Colen, I.; de Brito, J. Use of polycarbonate waste as aggregate in recycled gypsum plasters. *Materials* **2020**, *13*, 3042. [[CrossRef](#)]
21. Pedreño-Rojas, M.; Morales-Conde, M.; Pérez-Gálvez, F.; Rubio-De-Hita, P. Influence of polycarbonate waste on gypsum composites: Mechanical and environmental study. *J. Clean. Prod.* **2019**, *218*, 21–37. [[CrossRef](#)]
22. Yi, S.-Y.; Fan, L.-W.; Fu, J.-H.; Xu, X.; Yu, Z.-T. Experimental determination of the water vapor diffusion coefficient of autoclaved aerated concrete (AAC) via a transient method: Effects of the porosity and temperature. *Int. J. Heat Mass Transf.* **2016**, *103*, 607–610. [[CrossRef](#)]
23. Kang, Y.; Chang, S.J.; Kim, S. Hygrothermal behavior evaluation of walls improving heat and moisture performance on gypsum boards by adding porous materials. *Energy Build.* **2018**, *165*, 431–439. [[CrossRef](#)]
24. Bouzit, S.; Laasri, S.; Taha, M.; Laghzizil, A.; Hajjaji, A.; Merli, F.; Buratti, C. Characterization of Natural Gypsum Materials and Their Composites for Building Applications. *Appl. Sci.* **2019**, *9*, 2443. [[CrossRef](#)]
25. De Oliveira, K.A.; Barbosa, J.C.; Christoforo, A.L.; Molina, J.C.; Oliveira, C.A.B.; Bertolini, M.S.; Gava, M.; Ventrone, G. Sound absorption of recycled gypsum matrix composites with residual cellulosic pulp and expanded polystyrene. *BioResources* **2019**, *14*, 4806–4813.